PHOTOSYNTHETICA 43 (4): 519-528, 2005

Leaf anatomy, chloroplast ultrastructure, and cellular localisation of ribulose-1,5-bisphosphate carboxylase/oxygenase (RuBPCO) and RuBPCO activase in *Amaranthus tricolor* L.

J. HONG[*], D.-A. JIANG[**,***], X.-Y. WENG[**], W.-B. WANG[*], and D.-W. HU[*]

Institute of Biotechnology[*], State Key Laboratory of Plant Physiology and Biochemistry[**], College of Life Sciences, Zhejiang University, Hangzhou 310029, China

Abstract

In *Amaranthus tricolor* the leaf structure included three layers of chlorenchyma on the vascular bundle periphery, namely, mesophyll cells (MSCs) with few chloroplasts, outer larger round bundle sheath cells (BSCs) with many chloroplasts in a centripetal position, and inner smaller BSCs with few chloroplasts around the vascular bundle cells. The ultra-thin sections showed that BSCs had abundant organelles, namely many large and round mitochondria with well-developed cristae in the cytoplasm. The chloroplasts in the BSCs were lens-like bodies, which seemed to be oval on cross sections. Granal and intergranal thylakoids were usually distinguished. Grana were stacked in parallel with prevailing plane of thylakoid lamellae. The chloroplasts in the MSCs appeared smaller than those in the BSCs and contained less stacked thylakoids but abundant peripheral reticulum. The ultra-thin sections of immunogold-labelled anti-ribulose-1,5-bisphosphate carboxylase/oxygenase (anti-RuBPCO) exhibited high density of RuBPCO labelling in the stroma region of chloroplasts of the BSCs. Some anti-RuBPCO immunogold particles were observed in the stromal region of MSCs chloroplasts. The anti-activase (A) immunogold-labelling indicated that RuBPCOA was mainly distributed in the stroma region of both BSCs and MSCs chloroplasts. From the chloroplast ultrastructure and localisation of RuBPCO and RuBPCOA we deduced that the photosynthetic carbon reduction cycle and the formation of assimilatory power function in both MSC and BSC chloroplasts of *A. tricolor*.

Additional key words: grana; mitochondria; peripheral reticulum; thylakoids.

Introduction

C_4 plants exhibit specific anatomical, physiological, and biochemical characteristics. One particular anatomical feature of most C_4 leaves is presence of two kinds of distinct photosynthetic cells, mesophyll cells (MSCs) and bundle sheath cells (BSCs). In C_4 leaves the vascular bundles are close together. A tightly fitted BSCs containing many chloroplasts surround each bundle. Between the vascular bundles and adjacent to the air spaces of the leaf are the more loosely arranged MSCs (Hopkins and Hüner 2004). This distinct structural feature, called Kranz anatomy, plays a major role in C_4 plants. The key to the C_4 cycle is phospho*enol*pyruvate carboxylase (PEPC), which catalyses the carboxylation of PEP by using the bicarbonate ion HCO_3^- to form a moderately unstable product oxaloacetate (OAA) which is quickly either reduced to malate or transaminated to aspartate, both of which are more stable in MSC. Thereafter the more stable product is transported out of MSC into an adjacent BSC. Once in the BSC, the compound undergoes a decarboxylation with release of CO_2 that is re-fixed by RuBPCO into 3-PGA and reduced to triose. On the other hand, PEP regeneration occurs in MSCs. There are three photosynthetic types in C_4 plants depending on enzymes for catalyzing decarboxylation of organic acids in BSCs: NADP-malic enzyme (NADP-ME) type, in which OAA is first converted to malate that is then transported to the chloroplasts of BSC where it is decarboxylated to pyruvate and CO_2. The other two types are the NAD-malic

Received 25 January 2005, *accepted* 7 April 2005.
[***]Corresponding author; fax: +86(0)571-86971634; e-mail: <dajiang@zju.edu.cn>
Abbreviations: BS – bundle sheath; BSC – bundle sheath cell; ddH_2O – de-ionized distilled water; MS – mesophyll; MSC – mesophyll cell; OAA – oxaloacetate; PCK – PEP-carboxykinase; PCR – photosynthetic carbon reduction; PEP – phospho*enol*pyruvate; PEPC – PEP carboxylase; PGA – phosphoglycerate; RuBP – ribulose-1,5-bisphosphate; RuBPCO – ribulose-1,5-bisphosphate carboxylase/oxygenase; RuBPCOA – RuBPCO activase.
Acknowledgement: This work was partly supported by the National Natural Science Foundation (30471051, 39970440, 39970067) and the Doctoral Foundation of Education Department (20020335043) of P. R. China.

enzyme (NAD-ME) type and the PEP-carboxykinase (PCK) type, in which OAA undergoes a transamination reaction and the resulting aspartate is transported to the BSCs (Salisbury and Ross 1992). Decarboxylation in the PCK-type variant occurs also in the chloroplasts but in the NAD-ME variant the decarboxylating malic enzyme is located in the mitochondrion (Hopkins and Hüner 2004).

The different photosynthetic types are also distinguished by the even arrangement of chloroplasts in BSC. In the NADP-ME types and most of PCK types, the arrangement of chloroplasts in the BSC is centrifugal, while it is centripetal in the NAD-ME types. Lin *et al.* (1990) pointed out that the even arrangement of chloroplasts in BSCs may be an evolutional intermediate from centripetal (NAD-ME type) to centrifugal (NADP-ME and most PCK types) types.

Ribulose-1,5-bisphosphate carboxylase (RuBPCO) is photosynthetic key enzyme not only for C_3 plants but also for C_4 plants and its activation *in vivo* largely depends on RuBPCO activase (RuBPCOA) (Portis 1992, 1995, Portis and Salvucci 2002, Spreitzer and Salvucci 2002). Therefore RuBPCO and RuBPCOA localisations have been used to identify whether the PCR cycle functions in different green cells. RuBPCO is located in chloroplast pyrenoid of lower plants (Lacoste-Royal and Gibbs 1987, Osafune and Gibbs 1987, McKay and Gibbs 1991, Rawat *et al.* 1996, Borkhsenious *et al.* 1998) and in chloroplast stroma and/or thylakoid membrane regions of higher plants (Catherine *et al.* 1984, Caers *et al.* 1987, Shojima *et al.* 1987, Anderson *et al.* 1996, Nishioka *et al.* 1996, Miyake *et al.* 2001). In all C_4 types RuBPCO is located in BSC chloroplasts (Matsuoka *et al.* 2001). Recently, we have also reported the sub-cellular localisation of RuBPCO and RuBPCOA in rice (Wang *et al.* 2003), and barley and maize (Hong *et al.* 2004).

Amaranthus tricolor L., a vegetable widely cultivated in China, belongs to the NAD-ME photosynthetic subpathway of C_4 dicotyledons. Its quantum yield is 0.053 similar to 0.052±0.001 of C_3 species, but lower than 0.061±0.001 of the NADP-ME photosynthetic sub-pathway of C_4 species under normal atmospheric conditions and at leaf temperature of 30 °C (Ehleringger and Pearcy 1983). Its inner photosynthetic characteristic in different cell types is little known. The objective of our studies was to uncover those characteristics by observation of leaf anatomical structure, chloroplast ultrastructure, and RuBPCO and RuBPCOA localisation in the different cell types.

Materials and methods

Plants: *Amaranthus tricolor* L. was cultured in the greenhouse at the Huajiachi Campus of Zhejiang University. The plants used in experiments contained about ten leaves. The well-developed leaves were sampled, which were the 4th or 5th leaf counted from top to bottom of the plant.

Light microscopy: Leaf segments (1×3 mm) were fixed for 2 h at 4 °C in 0.1 M phosphate buffer (pH 7.2) containing 2.5 % (v/v) glutaraldehyde. They were post-fixed for 1 h at room temperature in the same buffer containing 1 % (m/v) osmium tetroxide, dehydrated through a gradient of ethanol series, and finally embedded in Spurr' resin. After polymerization the blocks were cut into 1 μm semi-thin sections with an ultramicrotome (*Reichert-Jung Ultracut E*). The semi-thin sections were smoothed out a slide and stained with 0.5 % toluidine blue solution. The leaf in cross section was observed and photographed under a microscope (*BH-2*, *Olympus*).

Electron microscopy: The same blocks were cut into 70 nm ultra-thin sections with the ultramicrotome. After staining the sections with uranyl acetate and lead citrate, cell ultrastructure was observed and photographed with an electron microscope (*JEM-1200EX*, *JEOL*).

Subcellular localisation of RuBPCO and RuBPCOA: Based on the method of Wang *et al.* (2003), the leaf blade was cut into pieces and fixed in 0.1 M phosphate buffer (pH 7.2) containing 3 % (v/v) paraformaldehyde and 1 % (v/v) glutaraldehyde for 2 h at 4 °C. After rinsing them in the same buffer (3–4 times, 15 min each), the pieces were dehydrated in an ethanol series and embedded in *Lowicryl K$_4$M* according to the following protocol: 100 % ethanol/resin (1 : 1, v/v) for 1 h, 100 % ethanol/resin (1 : 2, v/v) for 1 h, pure resin for 12 h at –20 °C. The embedded pieces were transferred to 0.5 cm^3 tubes filled with resin and polymerized completely under UV-radiation (λ = 360 nm) at –20 °C for 72 h, then at room temperature for 24 h. They were sectioned with an ultramicrotome. Ultra-thin sections were smoothly placed on the nickel grids. The grids were floated with section-side down toward the drops of de-ionised distilled water (ddH_2O) for 5 min, and then toward blocking liquid (BL; 0.05M PBS with 1 % bovine serum albumin, 0.02 % *PEG20000*, 0.1 M NaCl, 1 % NaN_3) for 30 min at room temperature. Then they were transferred to the drops of BL containing antibody to RuBPCO (1 : 800 dilution) or RuBPCOA (1 : 200 dilution) according to Wang *et al.* (2003), and incubated for 1 h. For control sections, antiserum was replaced with ddH_2O. The sections were washed in the drops of ddH_2O twice, 5 min for each, and incubated in BL containing protein A (secondary antibody)-15 nm colloidal gold particles for 1 h, and then in ddH_2O 3 times, 5 min each. The sections were subsequently stained with uranyl acetate and lead citrate, observed and photographed with an electron microscope (*JEM-1200EX, JEOL*) at 60 kV. The images were sam-

pled by *CIA-I* cell images analysis system. Area determinations and gold particle counts were made using *Cell Analysis* version *1.0* software to quantify RuBPCO and RuBPCOA (Wang *et al.* 2003). *T*-test was used to evaluate the differences in numbers of grana and immunogold labelling of RuBPCO and RuBPCOA in chloroplasts between the two cell types.

Results

Leaf anatomy: Transverse (Fig. 1*A*) and longitudinal (Fig. 1*B*) section of *A. tricolor* leaf showed BSC (pointed by *arrows*) around vascular bundle and BSC chloroplasts in centripetal arrangement. There was no obvious morphological difference in the mesophyll parenchyma cells between the upper and the lower epidermis (Fig. 1*A,B*). There were three layers of chlorenchyma on the vascular bundle periphery—one layer of mesophyll parenchyma cells and two layers of BSCs with chloroplasts (Fig. 1*C*). The outer layer of larger round BSCs had many chloroplasts arranged centripetally and the inner layer of smaller BSCs had few chloroplasts and/or mitochondria around the vascular bundle cells (Figs. 1*C* and 2*A*). Many mitochondria of a centripetal arrangement could be seen in the outer round BSCs (Fig. 1*C*) and they were close to chloroplasts. Many plasmodesmata (*arrow* in Fig. 1*E*) occurred in cell wall between BSCs and MSCs, implying extensive exchange of assimilates between the two cell types.

Ultrastructure of chloroplasts and mitochondria: The ultra-thin sections showed that the outer BSCs had abundant organelles (Figs. 1*C* and 2*A*). The cytoplasm was mainly distributed on the side near to vascular bundle and a large vacuole was located on the other cell side. There were many large and round mitochondria with well-developed cristae in the cytoplasm of BSCs (Fig. 1*D*). The chloroplasts in both outer and inner BSCs were lens-like bodies, except for smaller chloroplasts in the inner BSCs, which seemed to be oval on cross sections (Fig. 2*A*). Granal and intergranal thylakoids of the chloroplasts were usually distinguished. Grana were stacked in parallel with the prevailing plane of thylakoid lamellae (Fig. 2*B,C*). The MSC chloroplasts had less granal thylakoids but more peripheral reticulum (Fig. 2*D*). More-developed grana with an average of 4.87 thylakoids were found in the BSC chloroplasts and less-developed grana with an average of 3.13 thylakoids in the MSC chloroplasts (Table 1).

Immunolocalisation of RuBPCO in leaf cells: The anti-RuBPCO immunogold-labelled ultra-thin sections were observed by a transmission electron microscope. There were many gold particles (average density of 459 μm^{-2}) in the stromal region and only a few gold particles (average density of 46 μm^{-2}) in the granal region of BSC chloroplasts (Fig. 3*A,B*). Fig. 3*C* shows a large RuBPCO localisation in BSCs as well. Surprisingly some anti-RuBPCO immunogold particles were also observed in the stromal region of MSC chloroplasts although the average density of 166 μm^{-2} was not as high as that in the BSC chloroplast (Fig. 3*D,E*, Table 1). Few gold particles (average of 29 μm^{-2}) were found also in other organelles, including vacuole, nucleus, and mitochondria, and even in cell wall, but there was no difference in the density between the ultra-thin section regardless of treatment with or without RuBPCO antibody. Therefore the labelling of these regions might be non-specifically conjugated (Catherine *et al.* 1984, Borkhsenious *et al.* 1998, Miyake *et al.* 2001, Wang *et al.* 2003).

Table 1. Numbers of grana and immunogold labelling of RuBPCO and RuBPCOA in chloroplasts of two cell types of leaf in *Amaranthus tricolor*. *Anti-RuBPCO background value was 28.67±5.26, **anti-RuBPCOA background 17.20±4.72. ***Different letters show significant difference (p<0.01) between MSC and BSC. 30 chloroplasts forming 5–6 sections were observed randomly for every value.

		BSC	MSC
No. of thylakoids per granum		4.87±1.11 A***	3.13±0.86 B
No. of gold particles per stromal area [μm^2]	Anti-RuBPCO*	459.17±41.48 A	165.75±22.71 B
	Anti-RuBPCOA**	215.83±34.42 A	180.83±36.37 B

Immunolocalisation of RuBPCOA in leaf cells: The anti-RuBPCOA immunogold-labelling of ultra-thin sections under a transmission electron microscope illustrated chief distribution of gold particles in the stromal region of BSC (Fig. 4*A,B*) and MSC (Fig. 4*D,E*) chloroplasts of *A. tricolor*. The average density in BSC was 216 μm^{-2} and in MSC 180 μm^{-2}. Compared to the density in the granal region, the density in the stromal region was higher in both BSC and MSC chloroplasts (Table 1). The background in the other region of cell was only 17 μm^2 and the labelled particles were hardly observed in the ultra-thin sections without RuBPCOA antibody treatment. Fig. 4*C* indicates that RuBPCOA distribution in BSCi was significant.

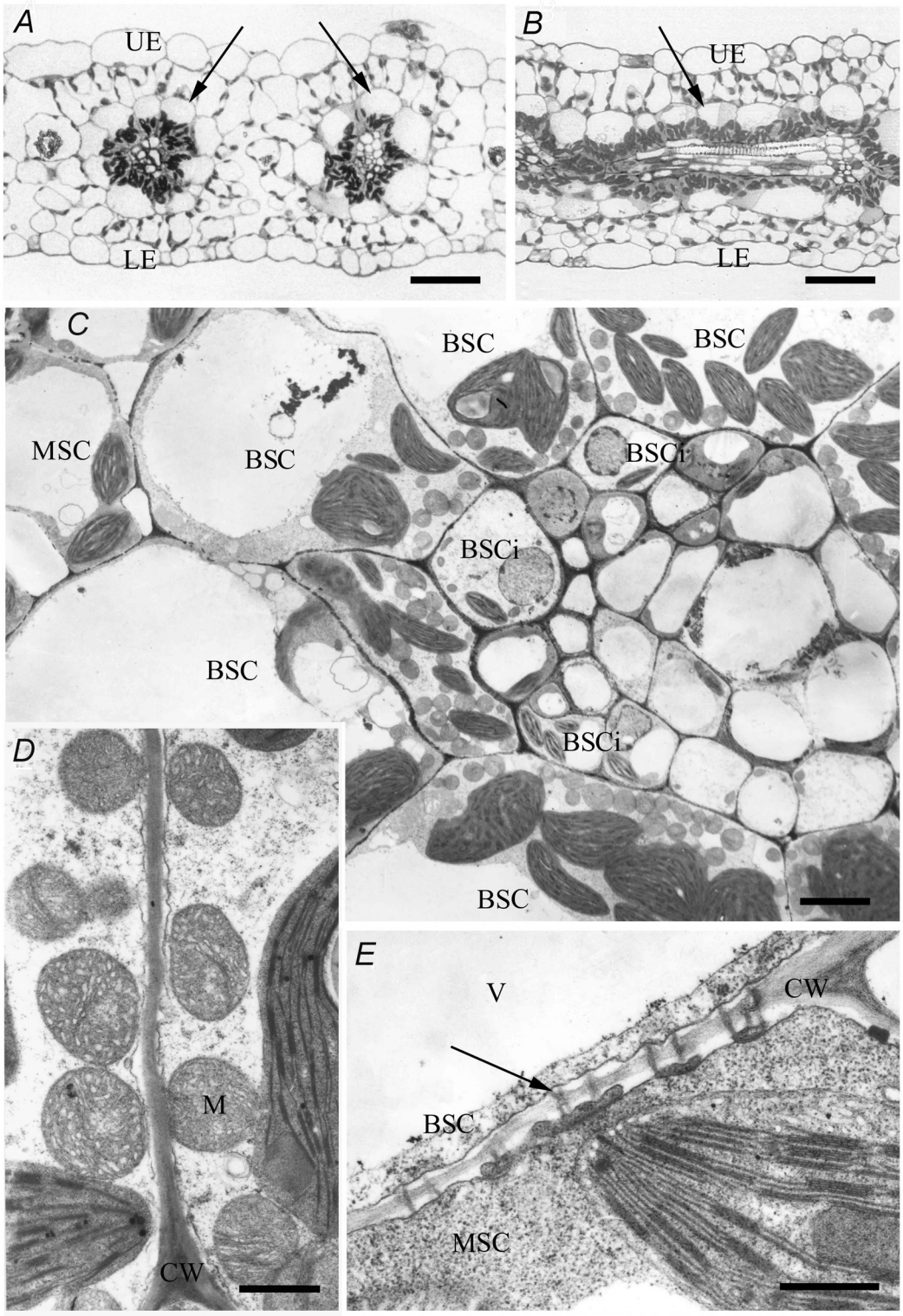

Fig. 1. Structure of leaf (*A*, *B*), vascular bundle (*C*), mitochondria (*D*), and plasmodesmata (*E*) in *A. tricolor*. Transverse (*A*) and longitudinal (*B*) sections show bundle sheath cells, BSCs (*arrows*) around vascular bundle and BSC chloroplasts in centripetal arrangement. *C*: Ultra-thin section of vascular bundle peripherals shows two layers of BSC, outer larger BSC with centripetally arranged chloroplasts and mitochondria, and inner smaller bundle sheath cell (BSCi) with a small number of chloroplasts. *D*: There are many well-developed mitochondria (M) in BSC. *E*: Many plasmodesmata (pointed by an arrow) exist in cell wall between BSC and mesophyll cell (MSC). *Bars* indicate 50 μm in *A* and *B*, 5 μm in *C*, and 500 nm in *D* and *E*. CW – cell wall, V – vacuole, UE – upper epidermis, LE – lower epidermis.

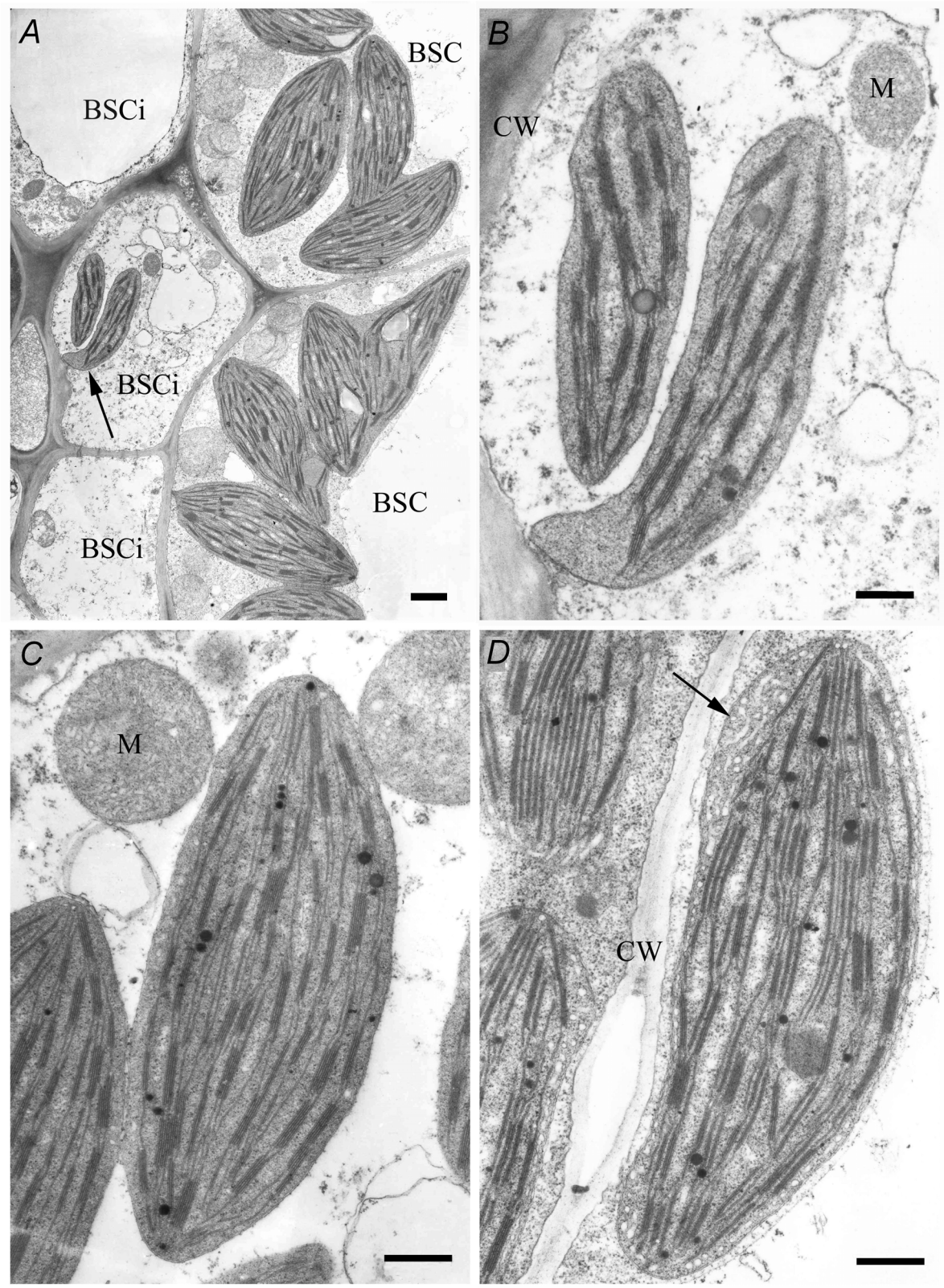

Fig. 2. The ultrastructure of chloroplasts in the BSC, the BSCi, and MSC (for abbreviations see Fig. 1). *A*: There are many larger chloroplasts in the BSC and some smaller chloroplasts in the BSCi (pointed by an *arrow*). *B*: Well-stacked grana chloroplasts exist in the BSCi. *C*: BSC chloroplasts have well-developed grana. *D*: MSC chloroplasts have less-stacked grana and some peripheral reticulum (*arrow*). *Bars* indicate 500 nm.

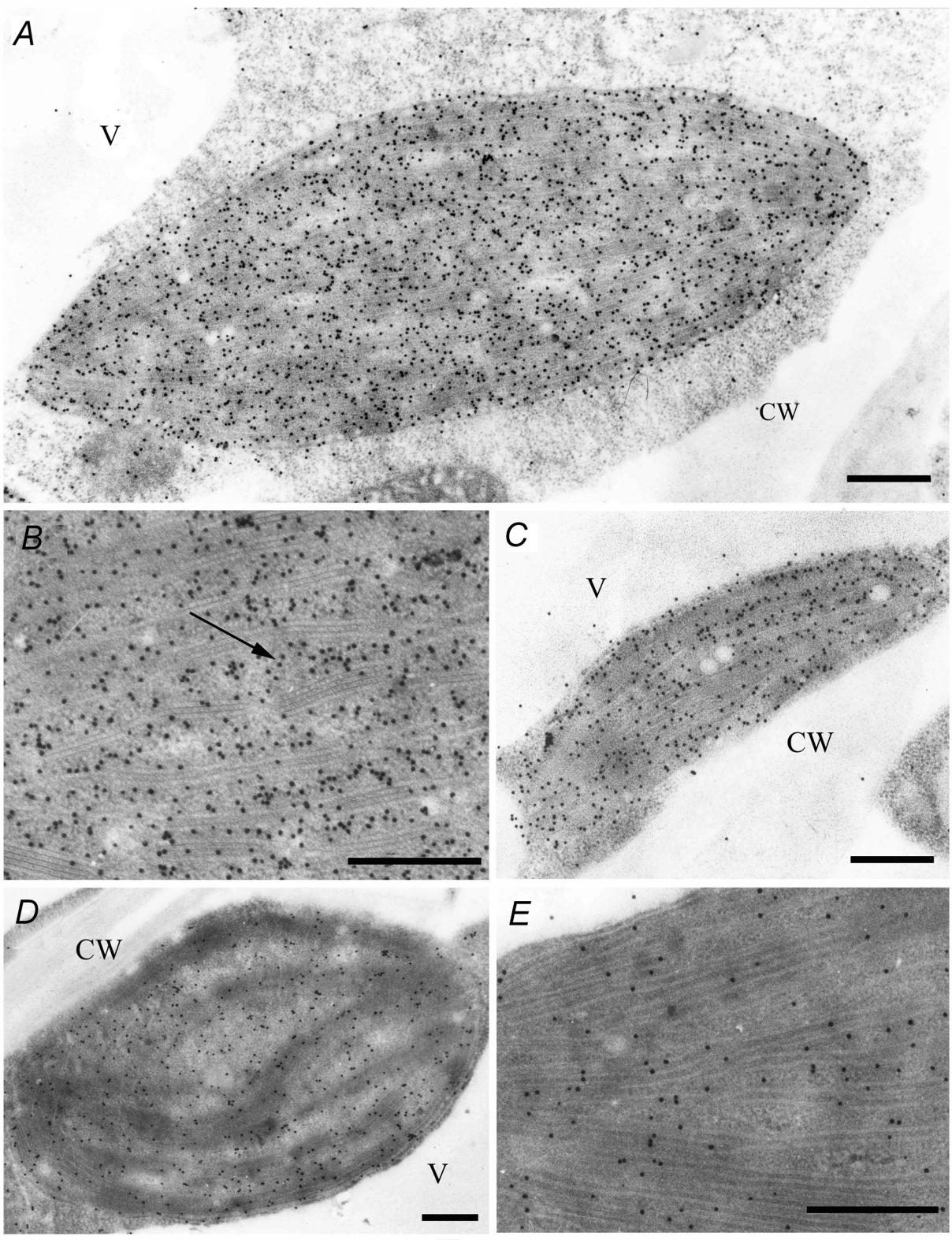

Fig. 3. Immunogold labelling of RuBPCO in the BS chloroplasts of *Amaranthus tricolor* leaf (for abbreviations see Fig. 1). *A*: Immunogold labelling is seen mainly in the BSC chloroplast. *B*: Immunogold particles of RuBPCO are localized to the stroma of the BSC chloroplast (*arrow*). *C*: Immunogold particles of RuBPCO are localized to the stroma of the BSCi chloroplast. *D*: Lower immunogold labeling density of RuBPCO exists in the MSC chloroplast. *E*: Less RuBPCO is localized to the stroma of the MSC chloroplast. *Bars* indicate 500 nm.

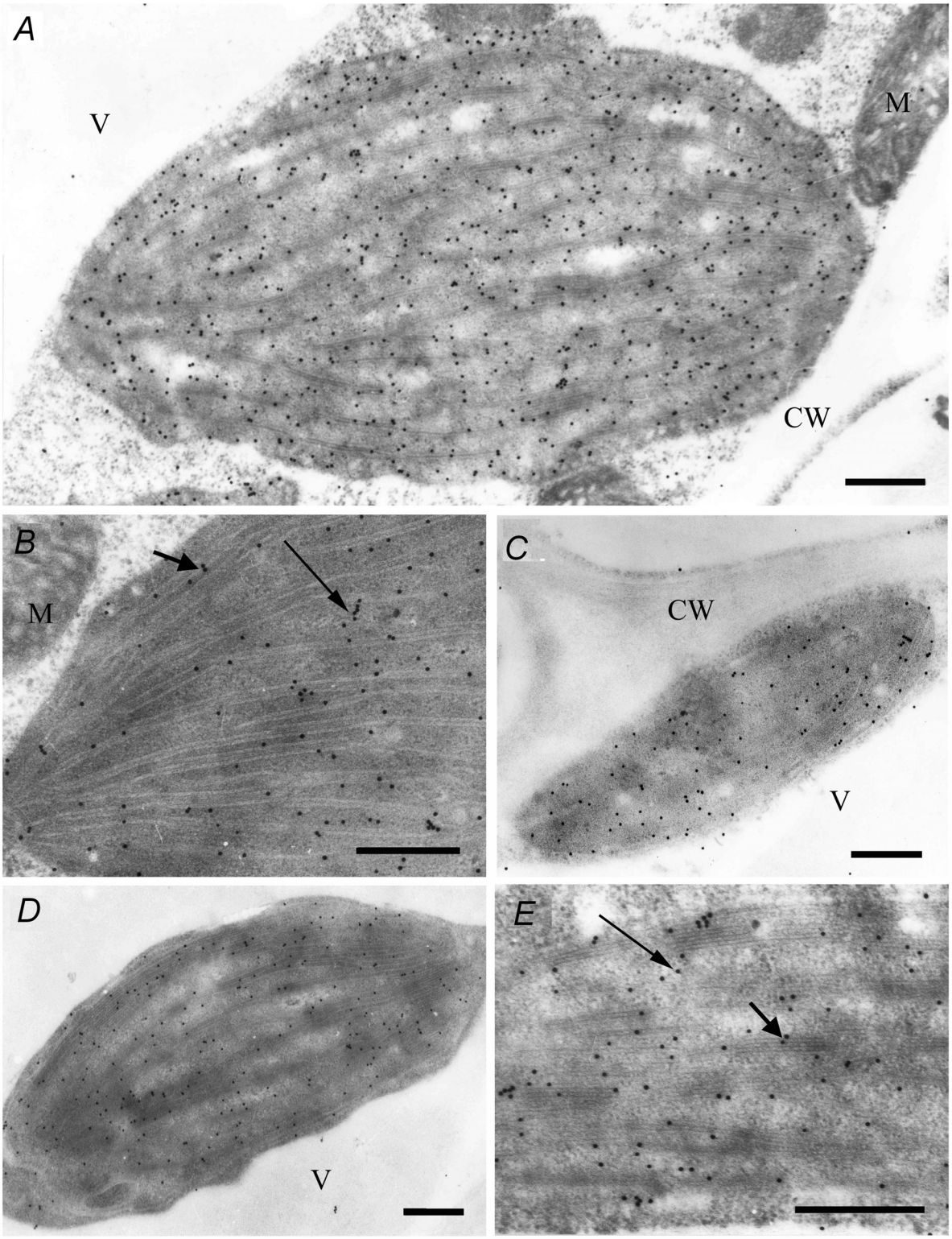

Fig. 4. Immunogold labeling of RuBPCOA in the BSC chloroplasts of *Amaranthus tricolor* leaf (for abbreviations see Fig. 1). *A*: Immunogold labelling of RuBPCOA exists in the BS chloroplast. *B*: Immunogold particles of RuBPCOA are localized to the stroma (*longer arrow*) and thylakoid membrane region (*shorter arrow*) of the BSC chloroplast. *C*: Immunogold particles of RuBPCOA are seen in BSCi chloroplast. *D*: Immunogold labelling of RuBPCOA exists in the MSC chloroplast. *E*: Immunogold particles of RuBPCO are localized to the stroma (*longer arrow*) and thylakoid membrane region (*shorter arrow*) of the MSC chloroplast. *Bars* indicate 500 nm.

Discussion

Since 1970s, many reports on C_4 leaf anatomy appeared (Olesen 1974, Sinha and Kellogg 1996, Fisher *et al.* 1997, P'yankov *et al.* 1997, Soros and Dengler 1998, Slaton and Smith 2002). Ultrastructure of maize chloroplast types has often been studied with regard to main photosynthetic activities (Pechová *et al.* 2003, Kutík *et al.* 2004); we reported the differences in chloroplast ultrastucture of barley and maize (Hong *et al.* 2004). In the present work, we found as a special feature of leaf anatomy in *A. tricolor* that individual BS consists of two layers of BSCs called the outer and inner BSCs, and one layer of MSCs in contact with the outer BSC (Fig. 1*A*,*B*). The outer BSCs looked larger, filled with organelles, and had much more chloroplasts and mitochondria in centripetal position, while the inner BSCs appeared more slender, with smaller and less abundant chloroplasts and mitochondria. We consider that the outer BSC is the dominant part for photosynthesis. In comparison with those in the MSC, chloroplasts in the *Amaranthus* BSC had more developed grana than in maize, an NADP-ME subtype, where the grana were hardly found in BSC chloroplasts (Hong *et al.* 2004). This might be explained by Osmond (1974) report that NAD-ME C_4 plants have both photosystems in the BSCs because these chloroplasts have well-developed grana (cf. Fig. 2*A–D* and Table 1). Our result that many mitochondria were close to chloroplasts in the BSC in *A. tricolor* (Fig. 1*D*) is in accordance with the finding that in the NAD-ME subtype the decarboxylating malic enzyme is located in the mitochondrion (Hopkins and Hüner 2004).

Several reports demonstrated that RuBPCO is dominantly distributed in plant organelles, which could participate in PCR, for instance, the pyrenoid of lower alga (McKay and Gibbs 1991, Borkhsenious *et al.* 1998). In a RuBPCO-deficient mutant of *Chlamydomonas reinhardtii* the existence of pyrenoid in cell could not be detected (Rawat *et al.* 1996). RuBPCO is located largely in chloroplasts of higher plants (Catherine *et al.* 1984, Caers *et al.* 1987, Shojima *et al.* 1987, Anderson *et al.* 1996, Nishioka *et al.* 1996, Miyake *et al.* 2001). It is widely accepted that RuBPCO and most other PCR cycle enzymes exist only in BSCs in C_4 plants and thus a complete PCR cycle occurs only in BSCs (Salisbury and Ross 1992, Matsuoka *et al.* 2001). Our results indicate that RuBPCO is localized in the stromal region of both MSC and BSC chloroplasts (Fig. 3*A–E*), implying that PCR cycle in *A. tricolor* is located in the MSCs.

Though RuBPCOA is an important enzyme activating RuBPCO *in vivo*, depending on the hydrolysis of ATP (Portis 1992, 1995, Salvucci and Ogren 1996) and perhaps playing other functions (Spreitzer and Salvucci 2002, Portis 2003), the reports on the cellular localisation of RuBPCOA are scarce. Anderson *et al.* (1996) found that RuBPCOA mostly exists in the stroma of chloroplast in pea, while Rokka *et al.* (2001) reported that the enzyme was largely distributed in the thylakoid membrane region and only scarcely in stroma. We also showed that RuBPCOA dominantly existed in chloroplasts and mitochondria of rice (Wang *et al.* 2003), and only in chloroplasts of barley and maize (Hong *et al.* 2004). The present experiment showed that RuBPCOA was localised in *A. tricolor* in both stromal and photosynthetic membrane regions of the BSC and MSC chloroplasts (Fig. 4*A–E*). But it was more distributed in the BSC chloroplasts than in the MSC chloroplasts and more in the stromal region than in the laminar region. The subcellular distribution of RuBPCOA is the same as that of RuBPCO, indicating the function of RuBPCOA to activate RuBPCO *in vivo*. Besides this function, RuBPCOA might play an important role in avoiding heat (Crafts-Brandner 1997, Crafts-Brandner and Law 2000) or other stresses (Pelloux *et al.* 2001), function as actin or chaperonin (Lilley and Portis 1997, Portis and Salvucci 2002, Spreitzer and Salvucci 2002, Portis 2003), and as the GA signal transduction component (Sharma and Komatsu 2002). Rokka *et al.* (2001) found that most of RuBPCOA was sequestered to the thylakoid membrane, particularly to the stroma-exposed regions during the first 10 min of heat treatment at 42 °C, and the association of RuBPCOA with the thylakoid membrane occurred more slowly at lower temperatures (38–40 °C). The temperature-dependent association of RuBPCOA with the thylakoid membrane was due to a conformational change in the RuBPCOA itself, not due to heat-induced alterations in the thylakoid membrane. Association of the 41 kDa isoform of RuBPCOA occurred first, followed by the binding of the 45 kDa isoform to the thylakoid membrane. It is still unclear whether RuBPCOA in the thylakoid membrane bears a specific function or just results from high temperature stress in the greenhouse where *A. tricolor* is planted.

Dimorphic chloroplasts exist in many C_4 plants, one type being MSC chloroplast with normal well stacked grana and few RuBPCO, and the other (BSC chloroplasts) with mostly unstacked thylakoids and low photosystem 2 and oxygen evolution activities, but normal RuBPCO content (Hong *et al.* 2004). Dimorphic chloroplasts imply the formation of most assimilatory power (ATP and NADPH) in the MSC chloroplasts and reaction of PCR cycle in the BSC chloroplasts. A part of 3-PGA must be transferred from the BSC chloroplasts to the MSC chloroplasts where it is reduced to glyceraldehyde-3-phosphate, which then returns to the BSC chloroplasts for regeneration of RuBP or accumulation of sugar. Therefore, the chloroplasts in BSC appear in centrifugal position and are close to those in the MSC in order to facilitate exchange of 3-PGA and glyceraldehyde-3-phosphate between the BSCs and MSCs. In our experiment, however, the chloroplasts in BSCs were arranged centripetally and were far away from the chloroplasts in MSCs

(Fig. 1*A,B*) which was more difficult for exchange of products between the BSCs and MSCs. The ultrastructure and RuBPCO and RuBPCOA localisation patterns are very similar in both cell types, and the NAD-ME subtype appears primary in evolution (Gutierrez *et al*. 1974, Lin *et al.* 1990). Therefore we suggest that in *A. tricolor* a complete photosynthetic process including the formation of assimilatory power and PCR cycle may be performed independently in both the MSC and BSC chloroplasts.

References

Anderson, L.E., Gibbons, J.T., Wu, W.X., Wang, W.X.: Distribution of ten enzymes of carbon metabolism in pea (*Pisum sativum*) chloroplasts. – Int. J. Plant Sci. **157**: 525-538, 1996.

Borkhsenious, O.N., Mason, C.B., Moroney, J.V.: The intracellular localization of ribulose-1,5-bisphosphate carboxylase/oxygenase in *Chlamydomonas reinhardtii*. – Plant Physiol. **116**: 1585- 1591, 1998.

Caers, M., Verbelen, J.P., Vendrig, J.C.: Ribulose-1,5-bisphosphate carboxylase and photosystem II activities during chloroplast development in mesophyll and bundle sheath cells of *Zea mays*. – Physiol. Plant. **70**: 68-72, 1987.

Catherine, P.R, Raymond, C., Pierre, G.: *In situ* immunofluorescent localization of phosphoenol pyruvate and ribulose-1,5-bisphosphate carboxylase in leaves of C_3, C_4, and C_3-C_4 intermediate *Panicum* species. – Planta **161**: 266-271, 1984.

Crafts-Brandner, S.J.: The two forms of ribulose-1,5-bisphosphate carboxylase/oxygenase activase differ in sensitivity to elevated temperature. – Plant Physiol. **114**: 439-444, 1997.

Crafts-Brandner, S.J., Law, R.D.: Effect of heat stress on the inhibition and recovery of the ribulose-1,5-bisphosphate carboxylase/oxygenase activation state. – Planta **212**: 67-74, 2000.

Ehleringger, J., Pearcy, R.W.: Variation in quantum yield for CO_2 uptake among C_3 and C_4 plants. – Plant Physiol. **73**: 555-559, 1983.

Fisher, D.D., Schenk, H.J., Thorsch, J.A., Ferren, W.R., Jr.: Leaf anatomy and subgeneric affiliations of C_3 and C_4 species of *Suaeda* (Chenopodiaceae) in north America. – Amer. J. Bot. **84**: 1198-1210, 1997.

Gutierrez, M., Gracen, V.E., Edwards, G.E.: Biochemical and cytological relationships in C_4 plants. – Planta **119**: 279-300, 1974.

Hong, J., Wang, W.B., Jiang, D.A., Hu, D.W.: [The immunogold localization of RuBPCO and its activase in chloroplasts of barley and maize leaves.] – J. Plant Physiol. mol. Biol. **30**: 561-568, 2004. [In Chin.]

Hopkins, W.G., Hüner, N.P.A.: Energy conservation in photosynthesis: assimilation. – In: Hopkins, W.G., Hüner, N.P.A. (ed.): Introduction to Plant Physiology. 3rd Ed. Pp. 89-123. John Wiley & Sons, Hoboken 2004.

Kutík, J., Holá, D., Kočová, M., Rothová, O., Haisel, D., Wilhelmová, N., Tichá, I.: Ultrastructure and dimensions of chloroplasts of leaves of three maize (*Zea mays* L.) inbred lines and their F_1 hybrids grown under moderate chilling stress. – Photosynthetica **42**: 447-455, 2004.

Lacoste-Royal, R.G., Gibbs, S.P.: Immunocytochemical localization of ribulose-1,5-bisphosphate carboxylase in the pyrenoid and thylakoid region of the chloroplast of *Chlamydomonas reinhardtii*. – Plant Physiol. **83**: 602-606, 1987.

Lilley, R.M., Portis, A.R., Jr.: ATP hydrolysis activity and polymerization state of ribulose-1,5-bisphosphate carboxylase oxygenase activase. Do the effects of Mg^{2+}, K^+, and activase concentrations indicate a functional similarity to actin? – Plant Physiol. **114**: 605-613, 1997.

Lin, Z., Shun, G., Li, S., Lin, G., Guo, J.: [The identification of photosynthetic subpathways of some C_4 and CAM plants.] – Acta bot. sin. **32**: 766-771, 1990. [In Chin.]

Matsuoka, M., Furbank, R., Fukayama, H., Miyao, M.: Molecular engineering of C_4 photosynthesis. – Annu. Rev. Plant Physiol. Plant mol. Biol. **52**: 297-314, 2001.

McKay, R.M.L., Gibbs, S.P.: Composition and function of pyrenoids: cytochemical and immunocytochemical approaches. – Can. J. Bot. **69**: 1040-1052, 1991.

Miyake, H., Nishimura, M., Takeoka, Y.: Immunogold labelling of RuBPCO in C_4 plant leaves for scanning electron microscopy. – Plant Product. Sci. **4**: 41-49, 2001.

Nishioka, D., Miyake, H., Taniguchi, T.: Suppression of granal development and accumulation of RuBPCO in different bundle sheath chloroplasts of the C_4 succulent plant *Portulaca grandiflora*. – Ann. Bot. **77**: 629-637, 1996.

Olesen, P.: Leaf anatomy and ultrastructure of chloroplasts in *Salsola kali* L. as related to the C_4-pathway of photosynthesis. – Bot. Notiser **127**: 352-363, 1974.

Osafune, R.G., Gibbs, S.P.: Immunogold localization of ribulose-1,5-bisphosphate carboxylase/oxygenase with reference to pyrenoid morphology in chroloplasts of synchronized *Euglena gracilis* cells. – Plant Physiol. **92**: 803-808, 1987.

Osmond, C.B.: Carbon reduction and photosystem deficiency in leaves of C_4 plants. – Aust. J. Plant Physiol. **1**: 41-50, 1974.

Pechová, R., Kutík, J., Holá, D., Kočová, M., Haisel, D., Vičánková, A.: The ultrastructure of chloroplasts, content of photosynthetic pigments, and photochemical activity of maize (*Zea mays* L.) as influenced by different concentrations of the herbicide amitrole. – Photosynthetica **41**: 127-136, 2003.

Pelloux, J., Jolivet, Y., Fontaine, V., Banvoy, J., Dizengremel, P.: Changes in RuBPCO and RuBPCO activase gene expression and polypeptide content in *Pinus halepensis* M. subjected to ozone and drought. – Plant Cell Environ. **24**: 123-131, 2001.

Portis, A.R., Jr.: Regulation of ribulose 1,5-bisphosphate carboxylase/oxygenase activity. – Annu. Rev. Plant Physiol. Plant mol. Biol. **43**: 415-437, 1992.

Portis, A.R., Jr.: The regulation of RuBPCO by RuBPCO activase. – J. exp. Bot. **46**(Special issue): 1285-1291, 1995.

Portis A.R., Jr.: RuBPCO activase – RuBPCO's catalytic chaperone. – Photosynth Res. **75**: 11-27, 2003.

Portis, A.R., Jr., Salvucci, M.E.: The discovery of RuBPCO activase – yet another story of serendipity. – Photosynth. Res. **73**: 257-264, 2002.

P'yankov, V.I., Voznesenskaya, E.V., Kondratschuk, A.V., Black, C.C., Jr.: A comparative anatomical and biochemical analysis in species with and without a Kranz type leaf anatomy: a possible reversion of C_4 to C_3 photosynthesis. – Amer. J. Bot. **84**: 597-606, 1997.

Rawat, M., Henk, M.C., Lavigne, L.L., Moroney, J.V.: *Chlamydomonas reinhardtii* mutants without ribulose-1,5-bisphosphate carboxylase/oxygenase lack a detectable pyrenoid. – Planta **198**: 263-270, 1996.

Rokka, A., Zhang, L., Aro, E.N.: RuBPCO activase: an enzyme with a temperature-dependent dual function. – Plant J. **25**: 463-471, 2001.

Salisbury, F.B., Ross, C.: Carbon dioxide fixation and carbohydrate synthesis. – In: Salisbury, F.B., Ross, C. (ed.): Plant Physiology. 4th Ed. Pp. 225-248. Wadsworth Publishing Company, Belmont 1992.

Salvucci, M.E., Ogren, W.L.: The mechanism of RuBPCO activase: Insights from studies of the properties and structure of the enzyme. – Photosynth. Res. **47**: 1-11, 1996.

Sharma, A., Komatsu, S.: Involvement of a Ca^{2+}-dependent protein kinase component downstream to the gibberellin-binding phosphoprotein, RuBPCO activase in rice. – Biochem. biophys. Res. Commun. **290**: 690-695, 2002.

Shojima, S., Nishizawa, N.K., Mori, S.: Do intrathylakoidal inclusions really contain RuBPCase? – Protoplasma **140**: 187-189, 1987.

Sinha, N.R., Kellogg, E.A.: Parallelism and diversity in multiple origins of C_4 photosynthesis in the grass family. – Amer. J. Bot. **83**: 1458-1470, 1996.

Slaton, M.R., Smith, W.K.: Mesophyll architecture and cell exposure to intercellular air space in alpine, desert, and forest species. – Int. J. Plant Sci. **163**: 937-948, 2002.

Soros, C.L., Dengler, N.G.: Quantitative leaf anatomy of C_3 and C_4 Cyperaceae and comparisons with the Poaceae. – Int. J. Plant Sci. **159**: 480-491, 1998.

Spreitzer, R.J., Salvucci, M.E.: RuBPCO: Structure, regulatory interactions, and possibilities for a better enzyme. – Annu. Rev. Plant Biol. **53**: 449-475, 2002.

Wang, N.Y., Jiang, D.A., Hong, J., Zhang, F., Weng, X.Y.: Diurnal changes of RuBPCO and RCA activities and their cellular localization in rice. – Acta bot. sin. **45**: 1076-1083, 2003.